Micó Vicent, B.; López-Herraiz, M.; Bello, A.; Martínez, N.; Martinez-Verdu, FM. (2017). Synthesis of pillared clays from metallic salts as pigments for thermosolar absorptive coatings. Solar Energy. 155:314-322. doi:10.1016/j.solener.2017.06.034

Synthesis of pillared clays from metallic salts as pigments for thermosolar absorptive coatings

Bàrbara Micó-Vicent[*a,b], María López-Herraiz[cd], Azucena Bello[c], Noelia Martínez[c], Francisco M. Martínez-Verdú[a].

[a]Colour and Vision Group, University of Alicante, Carretera de San Vicent, S/N, 03690, Spain.
[b]Departamento de Estadística e Investigación Operativas Aplicadas y Calidad, Universitat Politècnica de València (UPV), Plaza Ferrandiz y Carbonell 1, 03801, Alcoy, Alicante, Spain
[c]ABENGOA RESEARCH, Edificio Solandcenter, Carretera A-472, P.K. 5,85, margen derecha. 41800, Sanlúcar la Mayor (Seville), Spain
[d]Universidad Rey Juan Carlos. Paseo de la Castellana, 43. 28046 Madrid (Spain)
[*]Corresponding author. Tel.: +34 965903400 ext. 1162. E-mail address: barbara.mico@ua.es (http://web.ua.es/en/gvc).

Abstract

A general procedure for developing stable solar absorptive coatings at both high temperature and a high solar radiation concentration is presented. In order to generally improve thermal efficiency, a coating with high solar absorptance is applied all over the surface of receiver tubes that is subjected to extreme working conditions. Consequently, a durable coating with high absorptivity for sunlight is needed. An alternative paint formulation research and development line to Pyromark-2500, the paint currently used in many commercial solar thermal power plants (CSP) is proposed. Pigment synthesis is developed by intercalating metallic salts into laminar or tubular clay structures. Metallic oxides, which provide paint with its color properties, are obtained by a calcination process. Addition of silane or surfactants during the pigment synthesis is also optimized. Once dried and ground to a precise size, pigments are mixed with a commercial binder and applied to a metallic substrate to study their properties. Thermal stability to high temperature is studied with different tests. The results showed that laminar structure was preferred to intercalate larger amounts of metallic salt into the clay structure, and no significant differences were found when using silane or surfactant modifiers. Although the highest absorptivity value was 85% after 24 h at 600ºC, samples presented very good adherence to the metallic substrate. Addition of a small quantity of commercial black pigment to the paint composition could improve the absorptivity and maintain the excellent adhesion shown. Furthermore, montmorillonite clay, modified with a surfactant before adding metallic salt, and

CPS: solar thermal power plant
CPB: cetylpyridinum bromide
M: montmorillonite
L: laponite
HA: halloysite
SURF: surfactant
SIL: silane

without silane, resulted in a black pigment in a powder form. This pillared clay could be used in future paint formulations.

Keywords: Solar tower, coatings, pigments, optical properties, absorptivity

1. Introduction

In recent years, considerable efforts have been made to develop central receiver systems to harvest and convert sunlight into thermal energy and electricity. This energy source is enviro-friendly and reliable. The core component of a solar thermal power plant (CSP) is the receiver, which is coated with a highly absorptive coating. Searching for inexpensive optically efficient solar absorptive or selective coatings is a key factor in thermosolar energy applications.

This coating dramatically improves the energy collection yield of thermal solar collectors for thermal solar power plants. The coating is optimized to remain stable at high temperatures and to ensure long durability. By increasing both the energy collection yields of thermal solar power plants and the operating temperatures of power plants, it is possible to dramatically increase the efficiency of the solar to electric energy conversion rate [1-4].

Black paints are common coating materials for solar absorbers but, in the course of time, they have been gradually driven out of use and replaced with coatings prepared by other more sophisticated deposition methods; e.g., reactive sputtering, vacuum evaporation, electrochemical deposition and spraying colloidal solutions combined with post-treatment. Pyromark Series 2500 high temperature paint has been used on previous CSP central receivers and is considered a standard [5]. Pyromark-2500 is a relatively inexpensive, easy-to-apply coating with a solar absorptance of (0.96), but with high thermal emissivity (0.94).

The main reason for research not being intense on paints is that they are not solar-selective and their thermal emittance at working temperatures is around 0.90-0.94, which corresponds to high thermal radiation loss. Such loss is suppressed because, with thin absorbing layers, they are deposited on a metal substrate obtained by one of the above-mentioned techniques [6].

Typically when formulating paints, lots of challenges are faced in the system and formulation design as many components are involved in compositions. Paint components can be classified as four groups: binders, solvents, pigments and additives. Their composition and quantities depend on the application method, the desired properties, the substrate to be coated, and on ecological and economic constraints.

The most important component of a paint formulation is binders. Binders essentially determine the application method, drying and hardening behavior, adhesion to the substrate, mechanical properties, chemical resistance, and resistance to weathering [7].

Polyurethane/polyurea cross-linked binders confer the coating superior durability, mechanical strength and barrier properties [8]. Fluoropolymers could be another option to obtain coatings with excellent exterior durability, chemical resistance, good flexibility, good adhesion, little dirt retention, and good moisture and fungus resistance [9-12].

Pigments provide paint with color properties. One way of obtaining resistant pigments for extreme working conditions like high temperature, humidity, corrosion or thermal gradients is to use metal oxides as they present excellent chemical stability for the afore-mentioned conditions. Controlling oxide growth and disposition are key for controlling the optical properties of these natural pigments. One way of controlling oxide disposition is to use nanoclay as templates. Optical properties and color performance depend on nanoclay structures and the adsorption capacity of oxide precursors (metal salt solutions). Researchers have named composite materials (nanoclays and metal oxides) pillared clays. Laminar smectite clays (Montmorillonite or Laponite) or tubular-structured clays, such as halloysite, are used in ceramic industries as refractory materials, or as components when a thermal expansion risk is posed due to high temperatures as they present high thermal stability [13]. The literature focuses mainly on pillared clays for catalysis use, but these materials can also be used as pigments for coating formulations [14-16].

It is possible to change the color appearance of any metal oxide by simply changing the intercalation conditions [17]. Along these lines, our group is experienced in formulating hybrid composite-pigments based on organic dyes intercalated into laminar nanoclays to obtain a wide color gamut from the same organic dye [18, 19]. Black pigments from mixing different color pigments, e.g., dark yellows and blues, can be obtained. The objective of this work was to confer innovation to the synthesis of metal oxide hybrid composite-pigments using different nanoclay structures to improve their stability under working conditions with high solar absorptance for CSP applications. For this purpose, a preliminary design of the experiments was performed to discover the relevance of metal salt hybrid composite-pigments synthesis factors. These factors were nanoclay structure (size and shape) and two structural modifiers: surfactant and silane.

2. Experimental

2.1. Materials

Three different nanoclays, two with laminar cationic exchange capacity, montmorillonite (M) and laponite (L) (Rockwood additives) and a tubular nanoclay, halloysite (HA) (Sigma Aldrich), were used. As the nanoclay structural modifiers, surfactant Cetylpyridinuim bromide hydrate (98%) (CPB) and silane (3-Aminopropyl)trimethoxy-silane (97%) were employed, and both were acquired from Sigma Aldrich. Three metallic salts were used, Manganese(II) chloride

tetrahydrate (99%), Iron(III) chloride hexahydrate (>99%) and Cobalt(II) chloride hexahydrate (99%), which also came from Sigma Aldrich. To adjust pH during the synthesis process, the sodium hydroxide (NaOH) reagent agent (97%) was used.

2.2. Synthesis Method

Clays were initially dispersed at 1500 rpm for 24 h in distilled water at different concentrations: 21.43 g/L for L and 30g/L for M and HA. The concentration of metallic salt solutions depended on the nanoclay employed. For Cobalt and Iron salts, the concentration was $5.14 \cdot 10^{-03}$ M in distilled water when mixed with both M and HA, and $3.85 \cdot 10^{-02}$M with L. For Manganese solutions, the concentration was $6.21 \cdot 10^{-02}$ M when using both M and HA, and $4.62 \cdot 10^{-02}$ M with L. Salt exchange was performed in two steps, first stirring at 1500 rpm at room temperature for 1 h, and second at 600 rpm for 24 h. Afterward, samples were centrifuged to remove the remaining solvent. The percentage of intercalated and adsorbed salt was calculated from the UV-VIS absorption spectra of the supernatant, measured in a spectrophotometer Jasco V650. At this point, the metallic salt intercalated into the clay presented a paste format as distilled water still remained in the structure. This paste was re-dispersed at 400 rpm for 30 minutes to remove any possible traces of salt that did not intercalate into the clay structure. The washing process was run 3 times. The paste-hybrid composite-pigment was dried in an oven at 90 ºC for 24 h to obtain the pigment powder. Finally, metal oxides were obtained by a calcination process in a heating muffle at 800 ºC for 3 h in an oxidant atmosphere (Figure 1). The composite material that resulted from both the amorphous nanoclay structure and the generated metal oxides was finally called a hybrid composite-pigment. The final optical properties from the hybrid pigments could differ depending on synthesis conditions.

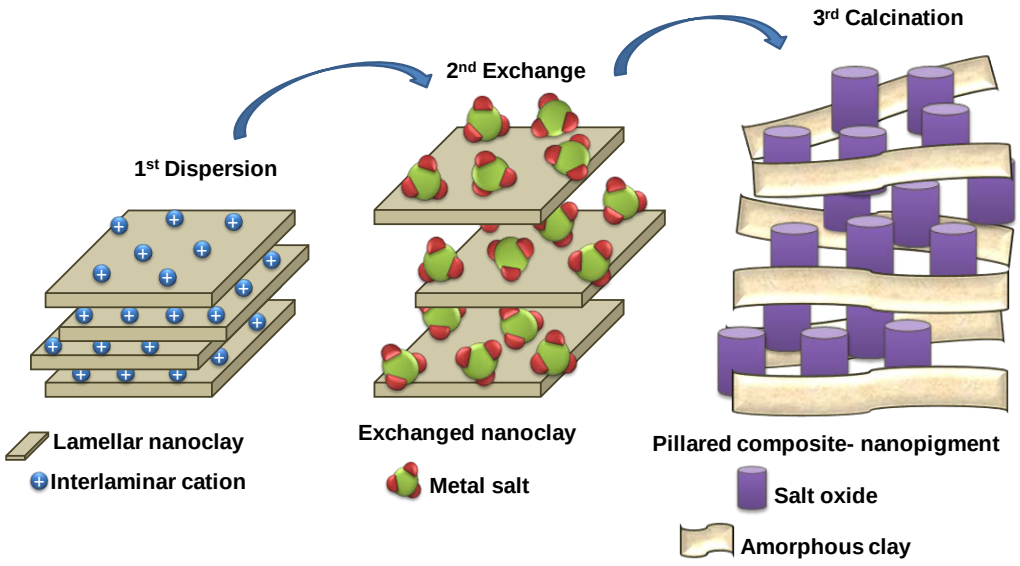

Figure 1. Synthesis method scheme of the new metal oxide-clay composite materials, or the hybrid composite-pigments from metal salts.

2.3. Design of Experiments (DoE)

Taguchi's (L9) DoE was used to study the effect of four synthesis factors with three levels on the obtained pillared nanoclays. The synthesis factors were: nanoclay (CLAY) with levels: 1-M, 2-L, 3-HA, surfactant (SURF), and silane (SIL) addition with levels: 1-Before addition of salt, 2-After addition of salt and 3-with no addition. The last factor was the hybrid pigment form (FORMAT) with only two levels: 1-calcinated and 2-the paste format. The nine experiments that resulted from this design (Table 1) were replicated in three blocks, one for each metal salt (Co, Fe, and Mn). The synthesis process yield was calculated from the metal salt concentration in the nanoclay structure after removing the supernatant during the washing process. The best color performance was expected to be obtained for the maximum amount of metallic salt intercalated into the clay structure.

Table 1. Experimental synthesis conditions for the L9 Taguchi's design for maximum metal salt adsorption at three clay levels (CLAY): laponite (1), montmorillonite (2), halloysite (3), three surfactant (SURF) and silane (SIL) levels depending on time point the addition took place; before (1) or after (3) the salt solution, or without addition (2). The hybrid composite-pigment format at two levels: calcinated 800 ^{o}C, 3 h (1), or the paste form (2).

Exp.	CLAY	SURF	SIL	FORMAT
1	2	2	1	2
2	1	2	3	2
3	2	3	3	1
4	1	3	2	2
5	3	1	3	2
6	2	1	2	2
7	3	2	2	1
8	1	1	1	1
9	3	3	1	2

2.4. Characterization techniques

Different characterization techniques were used to control the hybrid pigment properties. An X-ray photoelectron spectroscopy analysis was performed to characterize the oxidation states of

salts. Measurements were taken in a VG-Microtech Mutilab 3000 with pass energy from 2-200 eV, and an X-ray radiation source with the Mg and Al anodes. Supernatant solvent characterization was done in a transmission spectrophotometer Jasco V650 within the [190-870] nm range with a band increment ($\Delta\lambda$) of 0.5 nm. For the morphological characterization and structural properties of the hybrid composite-pigments, a transmission electron microscopy (TEM) (JEOL JEM-2010 model) was employed, at an image resolution of 0.38 between points and 0.2 nm between lines. Finally, in order to control the crystalline properties of nanoclays before and after treatments, DRX Bruker D8-Advance equipment, with a Göebel mirror (power: 3000 W, tension: 20-60 KV and current intensity: 5-80 mA), was used. Measurements were taken in an oxidant atmosphere at an angular speed of 1º/min, STEP 0.05º and an angular scan of [2.7-70]º.

The optical characterization of paints from UV to NIR was performed in a Lambda-1050 UV/VIS spectrometer (Perkin Elmer) with the WinLab Software. This spectrometer uses an integrating sphere attachment to measure reflectance. Absorptance is calculated by measuring the near UV, visible and IR from 300 nm to 2500 nm. Scans were run at a resolution of 10 nm increments with a monocromator change at 860.8 nm and a lamp change at 319.20. IR reflectance measurements are taken with a FTIR-Vertex 70 from 500 to 7000 cm^{-1} using an integrating sphere (Bruker A562) at the 15 cm^{-1} resolution. The diffuse and specular reflected part of light is detected by a detector located behind the outlet port.

3. Results and Discussion

3.1. XPS

The synthesis and oxidation processes of nanoclays intercalated with different metal salts into their structures were proved after the calcination process. The next results were taken only from the calcined hybrid composite-pigments. In the example provided with montmorillonite clay, salts were mixed individually and in pairs with the corresponding clay to study the intercalation process. The reason here was to understand the competition effect of the metal salt ions to be inserted into the clay structure and the formation of different mixed metal oxides in the nanoclay structure.

Figure 2 shows the O1s analysis, which corresponded to the montmorillonite intercalated with $FeCl_2$. A band with two peaks (B) at 532.17 eV and (A) at 529.83 eV was obtained, and indicated that the majority of oxygen present was bent in the OH-bond that corresponded to the montmorillonite structure. Most oxygen formed oxide O^{-2}. The Fe analysis (Figure 3) evidenced that spectra can be divided into two proportions (at about 710-712 and 725 eV, respectively). There was also a distinctive shake up satellite at around 719 eV. Presence of a peak on the BE curve at 710.2 eV was assigned to $Fe^{3+}2p_{3/2}$ and the second aforementioned

band was attributed to Fe $2p_{1/2}$ (725 eV). Therefore, the XPS studies indicated iron in the Fe^{3+} states and oxygen in the O^{2-} chemical states, which confirmed Fe_2O_3 formation.

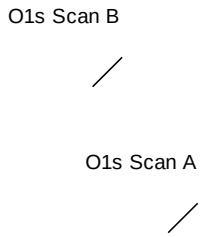

Figure 2. The XPS plot with deconvolution bands (A,B) for the O1s oxidation analysis.

The XPS analysis and deconvolution peaks (A, B or C) were performed for all the salts intercalated in the montmorillonite clay to identify the oxidation states of each element of the different salts after the calcination process. All the results are shown in Table 2.

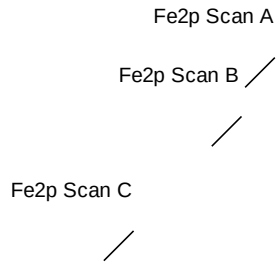

Figure 3. The XPS plot with deconvolution bands (A,B,C) for the Fe2p oxidation analysis

The intention was to combine the optical properties that each metallic oxide could provide the final pigment color with. Based on the results shown in Table 2, cationic selectivity during the intercalation process was evidenced as Fe ions were more easily intercalated into the laminar clay structure. The metal salt ratio of the ions intercalated between clay structures depends on the ion molecular radio. The amount of ions of the intercalated Fe was similar to the amount of ions of intercalated Mn. Therefore, the ionic radius of both should be similar. For Co ions, the intercalated amount was very small compared to that of Fe ions. The ionic radius of Co was only larger than the other two aforementioned ions if it was in a high spin state. The ionic radius

of Mn^{4+} with a coordination state of IV should be similar for Fe^{3+}. This result is possible only with a low spin state for Fe^{3+}.

Table 2. Identifications of oxides against the XPS peaks bands for montmorillonite adsorption of a single metal salt solution or of two different metal salt solutions.

Single Salt	**E(eV)**		**E(eV)**	**Oxides** [18, 20]
Mn2p A	641.35	O1s A	530.65	MnO_2
Mn2p B	643.02	O1s B	532.19	
Mn2p C	646.43	O1s C	535.36	
Two salts	**E(eV)**		**E(eV)**	**Oxides** [21-23]
Fe2p A	710.65	O1s A	530.55	Fe_2O_3
Fe2p B	713.25	O1s B	532.23	Co_2O_3
Fe2p C	719.50	O1s C	534.02	Ratio:
Co2p A	782.07			Fe=2.62Co
Co2p B	786.40			
Fe2p A	709.92	O1s A	530.29	Fe_2O_3
Fe2p B	712.81	O1s B	532.11	MnO_2
Mn2p A	640.51	O1s C	534.87	Ratio:
Mn2p B	642.59			Fe=1.17Mn
Mn2p A	641.30	O1s A	530.20	
Mn2p B	643.36	O1s B	532.00	MnO_2
Mn2p C	646.08	O1s C	534.12	
Co2p A	780.36			Co_2O_3
Co2p B	782.79			Ratio:
Co2p C	787.09			Mn=1.84Co

It was difficult to control the amount of each ion that inserted into the clay structure due to the competitiveness between the ions in the dissolution. For this reason, the experiment was designed with only one intercalated salt at a time.

3.2. UV-VIS Adsorption

Following the experimental conditions designed in Taguchi L9 (Table 1), the absorptance of the extracted solvent in the centrifuging step was measured for each hybrid pigment before the calcination step. To obtain a hybrid composite-pigment with strong dark colors, it is necessary to improve its absorption capacity. This was why the analysis was performed with all the synthesized hybrid composite-pigments using all the separated solvents after the centrifuging

process. Calibrations were performed using the UV-VIS adsorption spectra for the three metal salts. The aforementioned calibration curves were employed to calculate the salt concentration dissolved in the supernatant. The percentage of adsorbed salt in nanoclays was used as an optimization response in the DoE.

The analysis of variance (ANOVA) results are shown in Table 3. The only significant factor, where P-Value was under (0.05), was B: CLAY. This result indicates that, under the explained synthesis conditions, the factor that most influenced the metal salt intercalation (%) was the nanoclay structure.

Table 3. ANOVA for the adsorption response –sum of squares III type- using three blocks depending on the metal salt: $CoCl_2$ (1), $FeCl_3$ (2) and $MnCl_2$ (3).

Principal effects	Sum of Squares	l.g.[c]	Medium Squares	F-rate	P-Value
A:BLOCK	71.2554	2	35.6277	0.12	0.8842
B:CLAY	2226.23	2	1113.11	3.87	0.0400
C:SURF[a]	748.777	2	374.389	1.30	0.2965
D:SIL[b]	771.903	2	385.951	1.34	0.2863
RESIDUALS	5176.99	18	287.611		
TOTAL (CORRECTED)	8995.16	26			

[a] Surfactant factor
[b] Silane factor
[c] Degrees of freedom in the multifactorial ANOVA

Means plots were calculated to identify the effect of each factor on the adsorptions response. No significant difference between block levels (Figure 4) was found. This result indicates that there was no difference in the synthesis performance for all three metal salt molecules. Differences in nanoclay levels showed no distinction between laponite (1) or montmorillonite (2), but a significant difference appeared when halloysite was used (3). This result can be attributed to the fact that M and L have a laminar structure, while HA is arranged in a tubular structure. At this point, the best option to achieve a high salt intercalation content into clay is to use nanoclays with a lamellar structure instead of a tubular one. Based on the results, the use of montmorillonite is preferable. It is likely that the slight improvement in the salt intercalation obtained with M could correlate with this clay's laminar distance, which is more suitable for the metallic ions used in the experiments. Further results should be obtained if the ionic radius of the employed salt significantly differs from those mentioned herein.

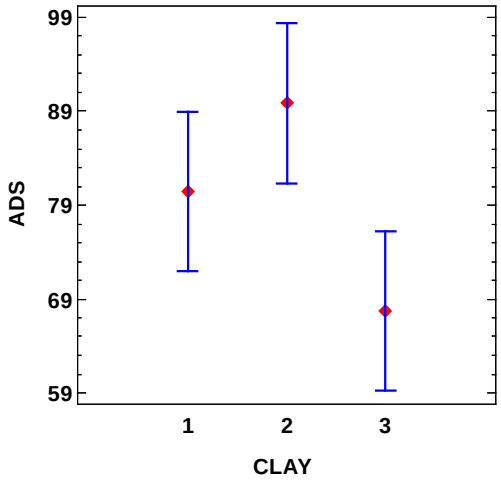

Figure 4. LSD Fisher means plot (95%) for effects of CLAY levels (laponite (1), montmorillonite (2) and halloysite (3)) on the maximum adsorption response (ADS).

The results concluded that the nanoclay used should be montmorillonite, and it is preferable to add the surfactant after mixing the metal salt solution with clay, and that silane should be added at the beginning of the process.

3.3. TEM

The transmission electron microscopy analysis of the salt hybrid composite-pigments was performed to control the morphological changes of nanoclays during the calcination process. It was necessary to use dyed samples (powder) to perform this analysis. Without salt intercalation, the three nanoclay structures were heat-treated at different temperatures, and then the microscopy analysis was performed. The Montmorillonite (Figure 5) and Laponite (Figure 6) structures underwent significant morphological changes after the calcination process. This calcination process was performed at different temperatures (600, 700 and 800 ºC) to study the thermal stability of the laminar structure of the system clay intercalated with metal oxides. As Figure 6 shows, it was impossible to maintain the laminar structure after performing the process at 600 ºC. Lowering the calcination temperature could lead to uncomplete oxidation formation. A similar result was obtained when studying Laponite. With the halloysite nanotubes (Figure 7), its tubular structure was maintained during the calcinations process. However, the XRD patterns then showed that the crystalline structure was lost at a temperature above 800 ºC.

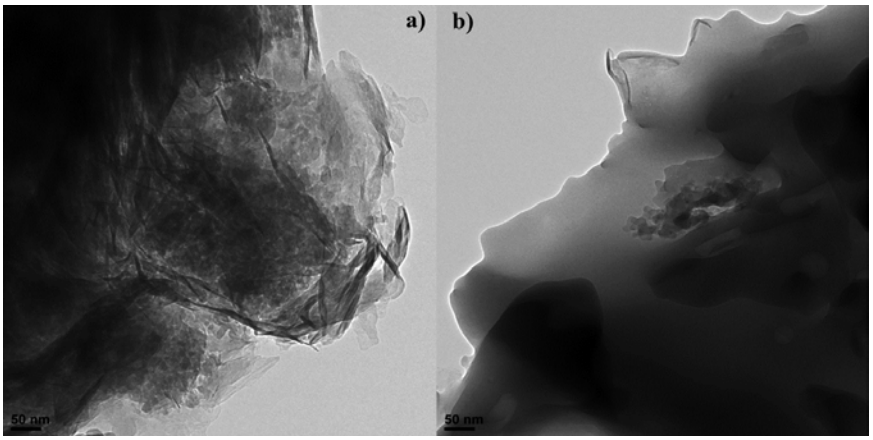

Figure 5. TEM images of the montmorillonite thermal treatments at 600ºC (a) and 800ºC (b).

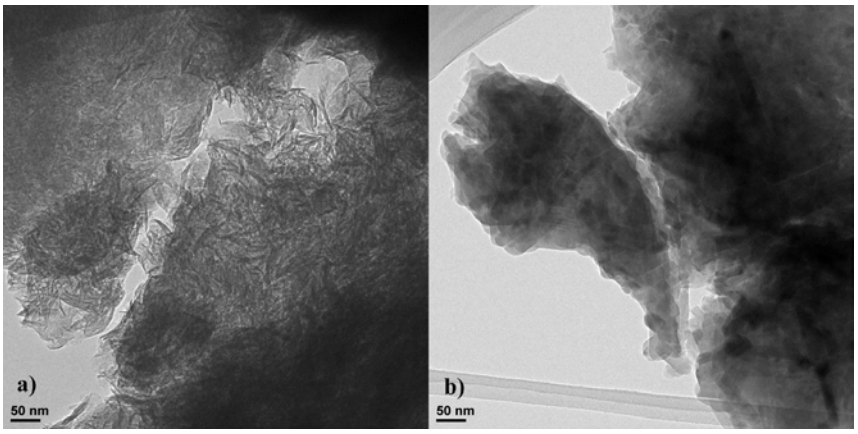

Figure 6. TEM images of the laponite thermal treatments at 600ºC (a) and 800ºC (b).

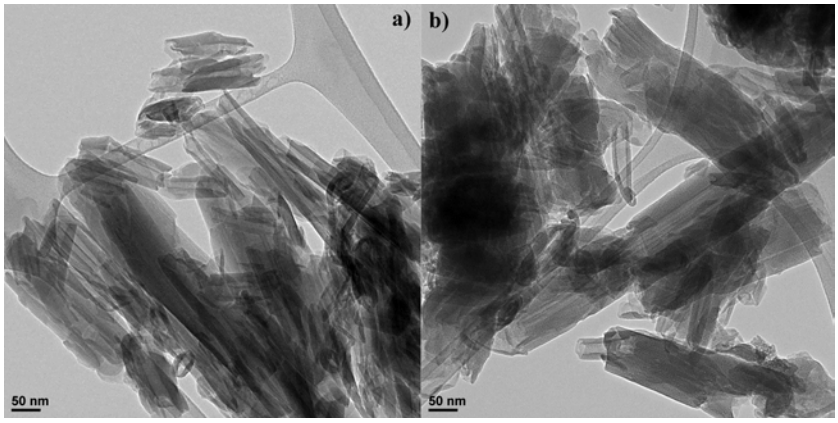

Figure 7. TEM images of the halloysite thermal treatments at 600ºC (a) and 800ºC (b).

3.4. XRD

The diffraction patterns of the hybrid composite-pigments dried in an oven at 100 ℃ before and after pigments were calcined at 800 ºC were analyzed. The diffraction peaks that corresponded to the interlaminar distance of nanoclays d(00l) were observed in the initial clay

spectra, which disappeared in the subsequent measurements that corresponded to the samples after both the intercalation and the calcination process (Figure 8). These results confirmed the structural change observed in the TEM analysis of the laminar nanoclays.

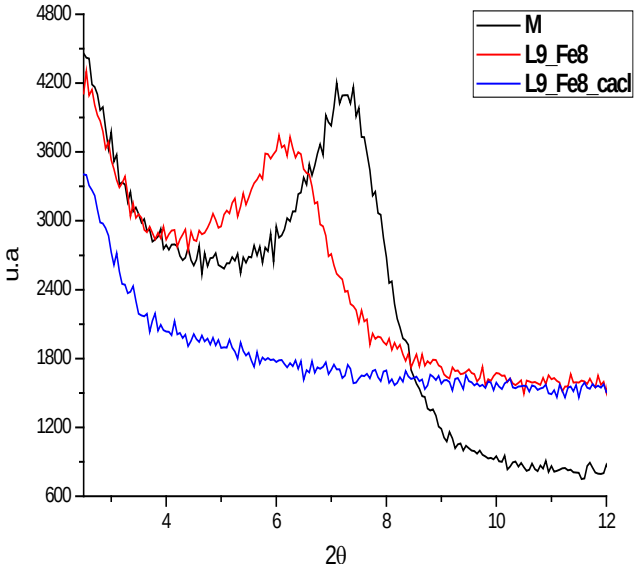

Figure 8. The XRD patterns of the initial montmorillonite (M) intercalated with $FeCl_3$ and treated at both 100ºC (L9_Fe8) and at 800ºC (L9Fe8_calc).

Based on these results, with a view to studying the thermal stability of the three clays selected herein, a heat treatment analysis was performed which used only the original nanoclays. Samples were subjected to different temperatures, ranging from 400 ºC to 1000 ºC. Figure 9 shows that the lamellar structure of montmorillonite or laponite was not maintained at temperatures above 800ºC. The halloysite nanotubes interaction was broken a temperatures above 400 ºC (Figure 10).

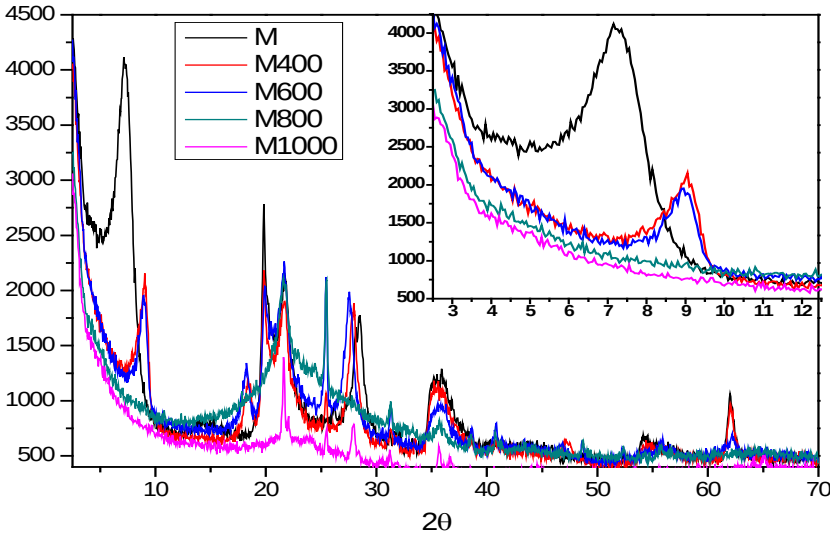

Figure 9. The XRD patterns of the original montmorillonite (M), and heat treated from 400 ºC to 1000 ºC (M400, M600, M800, M1000).

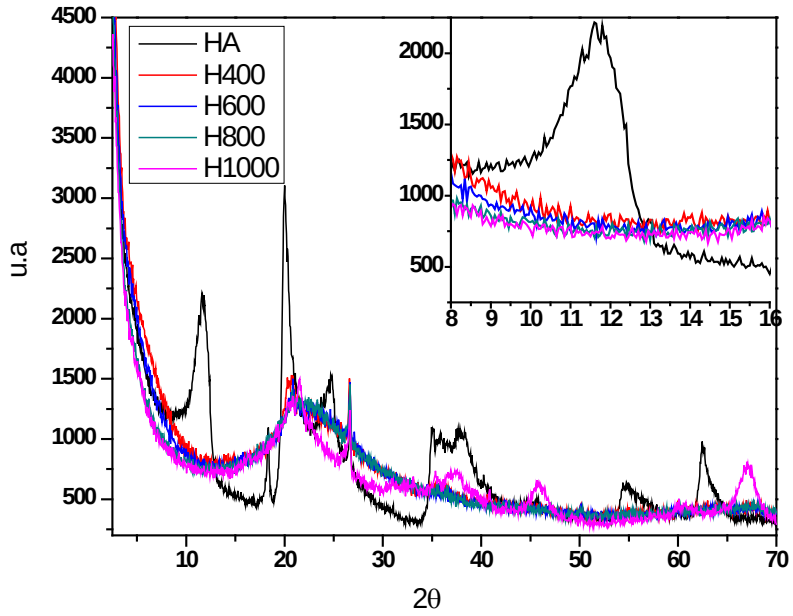

Figure 10. The XRD patterns of the original Halloysite (HA), and heat treated from 400 ºC to 1000 ºC (H400, H600, H800, H1000).

These results agree with previous research, which explains the crystalline structural modification of montmorillonite-type clay with temperature. At temperatures above 650º C, the dehydration process of the hydroxyl (OH^-) groups of the octahedral layers takes place. However the lamellar structure remains and Al(VI) turns into Al(IV) in the octahedral layers (1).

$$Al - O_4\,(OH)_2 \rightarrow Al - O_4 + H_2O \qquad (1)$$

At temperatures over 800 ºC, an amorphous silica structure is obtained in which the basal space typical of lamellar silicates does not appear in the spectra. Over 900 ºC, the diffraction pattern corresponds to the μ-cordierite structure ($Al_3Mg_2AlSi_5O_{18}$).

3.5. Formulation of paints and temperature resistance test

The color changes from the paste salt-hybrid composite-pigments form (Figure 12) to their powder form after calcination are shown in Figure 13. Using a heat resistant binder, hybrid pigments can be applied as a paint format to obtain color-resistant paints at high temperatures. The ideal hybrid composite-pigment would be that with high optical absorptivity. Therefore, here the intention was to obtain a black pigment that could provide the desired absorptivity and stability at high temperatures, and one that is needed in thermosolar technology.

It was impossible to mix the paste hybrid pigment format with the selected binder because of water incompatibility. Absorption α (%) and emittance ε (%) could be tested only from the calcinated pigments, from montmorillonite clay. The powder format samples were tested by formulating single and mixed hybrid pigments from three salts. Two mixed formulations were tested: Mix1 with 50 % of L9-Co8 (single cobalt oxide intercalated under Taguchi's conditions of experiment number 8) and 50 % of L9Fe8 (single iron oxide intercalated under Taguchi's conditions of experiment number 8), and Mix2 using 60 % of L9-Co8 and 40 % L9-Fe8.

Table 4. The thermal test results for the calcined hybrid composite-pigments from Montmorillonite with presence of the surfactant and silane (condition 8) for three metal salts, and for two mixtures.

	Initial values		20h - 500ºC		20h - 600ºC	
Name	α %	ε (500ºC) %	α %	ε (500ºC) %	α %	ε (600ºC) %
L9Co8	84.39	94.3	84.2	94.2	83.4	94.2
L9Fe8	85.28	94.4	84.4272	94.2	84.8	94.3
L9Mn8	81.15	94.3	80.3385	94.2	80.2	94.2
UA-Mix1	84.19	94.5	83.3481	94.3	79.9805	94.5
UA-Mix2	84.8	94.7	83.952	94.5	80.56	94.6

Table 4 provides the thermal resistance test results after 20 h at 500 ºC and 600 ºC for the selected coatings. The best result was obtained with pigment L9Fe8. In any case the absorptivity values were high enough to be considered an alternative to Pyromark-2500. The main parameter that improved, compared to Pyromark-2500, was adherence. It was measured following Standard ISO 1518-1, where scale factors vary from 0-5, with 0 indicating the best adherence. This test was performed with the initial samples and with those thermally tested at 500 ºC and 600 ºC. Hybrid composite-pigments were mixed with the selected binder and stirred in a magnetic stirrer for over 1 h. The selected application method was paint-brush. Other application methods can also be applied, such as spraying, but this step was not optimized. After the curing step carried out in an oven, adhesion to the substrate was measured by standard specifications. Despite being somewhat subjective, it is well-accepted by the scientific community. In all cases, the tested samples could be attributed a value of 0, which proved good

coating adherence. The same procedure was carried out previously with Pyromark-2500 samples, and all test values were worst: 1-2 scale values. Figure 11 shows an example test made with Pyromark-2500 with scale value:2, and L9Fe8 with scale value of 0.

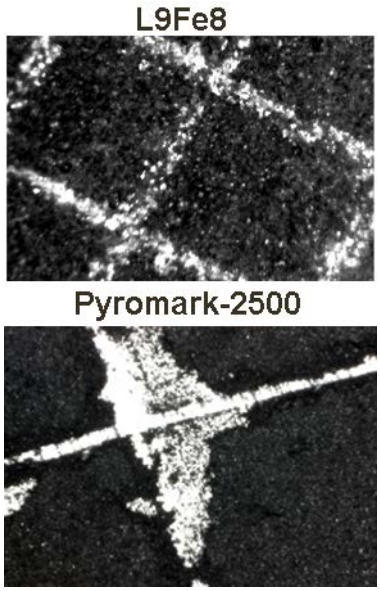

Figure 11. Standard ISO 1518-1 test example with Pyromark-2500 with scale value:2, and L9Fe8 with scale value of 0.

Accordingly, the experiment that achieved the best result was that obtained from manganese salt under experimental condition 6 (montmorillonite clay, modified before with the surfactant and without silane modification). Under this condition, the montmorillonite nanoclay was used in its modified form before adding manganese salt with the surfactant and without using silane (Figure 14). In order to improve the coating's absorptivity, a small proportion of commercial black pigments can be used in the composition.

Figure 12. Paste format of hybrid composite-pigments before heat treatment. From left to right: hybrid pigments from Fe, Co and Mn salts.

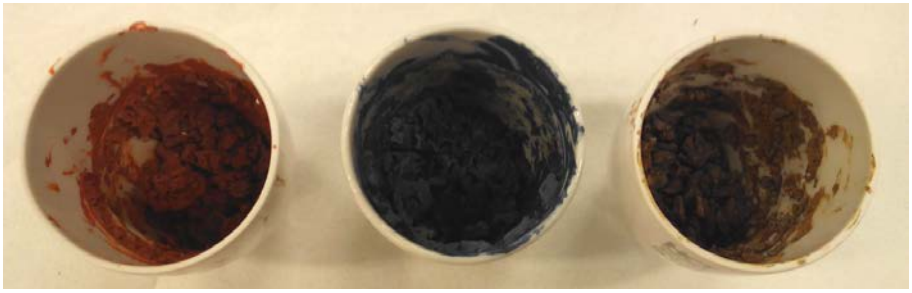

Figure 13. Powder-format of hybrid composite-pigments after heat treatment (800 ºC, 3h). From left to right: pigments from Fe, Co and Mn salts.

Figure 14. Calcinated hybrid composite-pigment (800 ºC, 3h) of the montmorillonite clay modified before adding manganese salt with the surfactant (L9-Mn6).

4. Conclusions

Pillared composite-clays proved suitable for synthesizing pigments, and displayed sound stability and excellent adhesion to metallic substrates. Two laminar clays and one tubular structure clay were used to force the molecule salts inserted into the structure to be guided following nanoclays patterns. In spite of nanoclay structure decompositions after the calcination process, the generation of metal oxides differed depending on synthesis process factors. These factors changed the nanoclay basal space and the lamellar or nanotubes distribution. As a result, the template effect from nanoclays was variable. Accordingly, different colors were obtained based on the various variables studied: clay, salt and additives. The DoE analysis concluded that the optimum conditions in salt-hybrid composite-pigments synthesis do not depend on the metal salt nature, but on the nanoclay structure. We found that the optimum conditions were montmorillonite clay modified only with the surfactant before adding salt. Metallic oxides formations were confirmed by XPS. Paints were developed and tested by mixing synthesized pigments with a commercial binder. Absorptivity was maintained after 20 h at 500ºC and 20 h at 600 ºC, which evidenced the stability of pigments. To improve absorptivity, darker paints can be made by adding a small quantity of commercial black pigment.

5. Future work

In future works, hybrid composite-pigments with higher absorptivity values should be found by mixing other metal ions or by completing further experiments with an extended Taguchi's

DoE. Focus should lie on the best conditions mentioned herein. A high temperature-resistant binder should improve the formulations under thermosolar receiver working conditions.

6. Acknowledgement

The research that has led to these results was funded by Abengoa Solar New Technologies S.A. by a private contract with the Colour and Vision Group of the University of Alicante.

7. Bibliography

[1] C.M. Lampert, Advanced optical materials for energy efficiency and solar conversion, Solar & Wind Technology, 4 (1987) 347-379.
[2] Z. Crnjak Orel, Characterisation of high-temperature-resistant spectrally selective paints for solar absorbers, Solar Energy Materials and Solar Cells, 57 (1999) 291-301.
[3] G. Smith, A. Gentle, P. Swift, A. Earp, N. Mronga, Coloured paints based on coated flakes of metal as the pigment, for enhanced solar reflectance and cooler interiors: description and theory, Solar energy materials and solar cells, 79 (2003) 163-177.
[4] M.K.e. Gunde, Z.C. Orel, M.G. Hutchins, The influence of paint dispersion parameters on the spectral selectivity of black-pigmented coatings, Solar energy materials and solar cells, 80 (2003) 239-245.
[5] C.K. Ho, A.R. Mahoney, A. Ambrosini, M. Bencomo, A. Hall, T.N. Lambert, Characterization of Pyromark 2500 paint for high-temperature solar receivers, Journal of Solar Energy Engineering, 136 (2014) 014502.
[6] B. Orel, H. Spreizer, L. Slemenik Perše, M. Fir, A. Šurca Vuk, D. Merlini, M. Vodlan, M. Köhl, Silicone-based thickness insensitive spectrally selective (TISS) paints as selective paint coatings for coloured solar absorbers (Part I), Solar Energy Materials and Solar Cells, 91 (2007) 93-107.
[7] Q. Geng, Optimization design of CuCrxMn2-xO4-based paint coatings used for solar selective applications, (2012).
[8] F. Levine, J. La Scala, W. Kosik, Properties of clear polyurethane films modified with a fluoropolymer emulsion, Progress in Organic Coatings, 69 (2010) 63-72.
[9] K.A. Wood, Optimizing the exterior durability of new fluoropolymer coatings, Progress in Organic Coatings, 43 (2001) 207-213.
[10] R.A. Iezzi, S. Gaboury, K. Wood, Acrylic-fluoropolymer mixtures and their use in coatings, Progress in Organic Coatings, 40 (2000) 55-60.
[11] K. Motohashi, N. Miyazaki, DURABILITY OF COATING MATERIALS MADE OF ANEW TYPE OF FLUOROPOLYMER CURED AT ROOM TEMPERATURE, in: Proceedings of the Fourth International Conference on Durability of Building Materials and Components, Pergamon, 1987, pp. 317-324.
[12] J. Scheirs, S. Burks, A. Locaspi, Developments in fluoropolymer coatings, Trends in polymer science, 3 (1995) 74-82.
[13] P. Wu, H. Wu, R. Li, The microstructural study of thermal treatment montmorillonite from Heping, China, Spectrochimica Acta Part A: Molecular and Biomolecular Spectroscopy, 61 (2005) 3020-3025.
[14] S. Li, P. Wu, H. Li, N. Zhu, P. Li, J. Wu, X. Wang, Z. Dang, Synthesis and characterization of organo-montmorillonite supported iron nanoparticles, Applied Clay Science, 50 (2010) 330-336.
[15] G. Montes-Hernandez, J. Pironon, F. Villieras, Synthesis of a red iron oxide/montmorillonite pigment in a CO2-rich brine solution, Journal of Colloid and Interface Science, 303 (2006) 472-476.

[16] Y.-H. Zhao, Q.-Q. Hao, Y.-H. Song, W.-B. Fan, Z.-T. Liu, Z.-W. Liu, Cobalt Supported on Alkaline-Activated Montmorillonite as an Efficient Catalyst for Fischer-Tropsch Synthesis, Energy & Fuels, 27 (2013) 6362-6371.
[17] G. Carbajal-Franco, M. Eastman, C.V. Ramana, Structure and optical properties of iron oxide films prepared by a modified wet-chemical method, Ceramics International, 39 (2013) 4581-4587.
[18] H. Seyama, Y. Tani, N. Miyata, M. Soma, K. Iwahori, Characterization of pebble surfaces coated with biogenic manganese oxides by SIMS, XPS and SEM, Applied Surface Science, 255 (2008) 1509-1511.
[19] Z.C. Orel, M.K. Gunde, M.G. Hutchins, Spectrally selective solar absorbers in different non-black colours, Solar energy materials and solar cells, 85 (2005) 41-50.
[20] M. Ferrandon, J. Carnö, S. Järås, E. Björnbom, Total oxidation catalysts based on manganese or copper oxides and platinum or palladium I: Characterisation, Applied Catalysis A: General, 180 (1999) 141-151.
[21] M. Aronniemi, J. Sainio, J. Lahtinen, XPS study on the correlation between chemical state and oxygen-sensing properties of an iron oxide thin film, Applied Surface Science, 253 (2007) 9476-9482.
[22] D.S. Petrovič, D. Mandrino, XPS characterization of the oxide scale on fully processed non-oriented electrical steel sheet, Materials Characterization, 62 (2011) 503-508.
[23] A.A. Khassin, T.M. Yurieva, V.V. Kaichev, V.I. Bukhtiyarov, A.A. Budneva, E.A. Paukshtis, V.N. Parmon, Metal–support interactions in cobalt-aluminum co-precipitated catalysts: XPS and CO adsorption studies, Journal of Molecular Catalysis A: Chemical, 175 (2001) 189-204.